



**Geometric morphometrics as a tool  
to support taxonomic identification in palaeontology:  
A comparison with traditional morphometrics  
in the study of isolated fossil shark teeth**

**Edoardo Pagliuzzi, Giorgio Carnevale, Jürgen Kriwet, and Giuseppe Marramà**

**ABSTRACT**

Isolated teeth of elasmobranch fishes are extremely abundant in the fossil record. However, taxonomic identification solely based on qualitative characters might lead to erroneous results because several taxa might exhibit similar morphologies, making it difficult to detect significant morphological differences. As a valid support for qualitative taxonomic identification, an increasing number of studies have proposed supplementing qualitative features with quantitative approaches, including both traditional and geometric morphometrics. These methods are particularly effective in detecting minimal morphological differences that are often overlooked by purely qualitative analyses. To evaluate whether traditional and geometric morphometric approaches can reliably support the qualitative taxonomic identifications, using geometric morphometrics we examined a sample of isolated teeth of living and fossil lamniform sharks that had been previously investigated using traditional morphometric approaches. The goal of the present study is to understand whether geometric morphometrics and traditional morphometrics, when applied on the same dataset of isolated shark teeth, are equally reliable in supporting a priori qualitative taxonomic identifications and, if so, which approach is more effective. Our results show that geometric morphometrics recovers the same taxonomic separation identified by traditional morphometrics while also capturing additional shape variables that traditional methods did not consider. Consequently, geometric morphometrics provides a larger amount of information about tooth morphology, representing a powerful tool for supporting taxonomic identification of isolated fossil shark teeth.

Edoardo Pagliuzzi. Dipartimento di Scienze della Terra, Università degli Studi di Torino, Via Valperga Caluso 35, 10125 Torino, Italy (corresponding author). [edoardo.pagliuzzi@edu.unito.it](mailto:edoardo.pagliuzzi@edu.unito.it)  
Giorgio Carnevale. Dipartimento di Scienze della Terra, Università degli Studi di Torino, Via Valperga

Final citation: Pagliuzzi, Edoardo, Carnevale, Giorgio, Kriwet, Jürgen, and Marramà, Giuseppe. 2025. Geometric morphometrics as a tool to support taxonomic identification in palaeontology: A comparison with traditional morphometrics in the study of isolated fossil shark teeth. *Palaeontologia Electronica*, 28(2):a33.

<https://doi.org/10.26879/1567>

[palaeo-electronica.org/content/2025/5603-geometric-morphometrics-on-fossil-shark-teeth](http://palaeo-electronica.org/content/2025/5603-geometric-morphometrics-on-fossil-shark-teeth)

Copyright: July 2025 Society of Vertebrate Paleontology.

This is an open access article distributed under the terms of the Creative Commons Attribution License, which permits unrestricted use, distribution, and reproduction in any medium, provided the original author and source are credited.  
[creativecommons.org/licenses/by/4.0/](http://creativecommons.org/licenses/by/4.0/)

Caluso 35, 10125 Torino, Italy. giorgio.carnevale@unito.it

Jürgen Kriwet. Department of Palaeontology, University of Vienna, Josef-Holaubek-Platz 2, 1090 Vienna, Austria. juergen.kriwet@univie.ac.at

Giuseppe Marramà. Dipartimento di Scienze della Terra, Università degli Studi di Torino, Via Valperga Caluso 35, 10125 Torino, Italy. giuseppe.marrama@unito.it

**Keywords:** lamniform sharks; fossil teeth; geometric morphometrics; traditional morphometrics; taxonomy

Submission: 16 April 2025. Acceptance: 14 July 2025.

---

## INTRODUCTION

Sharks (Selachii) are a successful group of marine vertebrates, with at least 500 living species worldwide distributed from the coastal shallow to cooler deep waters (Dulvy et al., 2014). They are characterized by a high dental morphological diversity that reflects their ability to adapt to different habitats and ecological niches (Pimiento et al., 2019). The evolutionary success of the sharks is also reflected by their very long evolutionary history and rich fossil record, which includes more than 3000 extinct species (Cappetta, 2012; Paillard et al., 2021), demonstrating that these organisms were able to survive several mass extinctions and overcome the competition with other marine predators.

Like other chondrichthyan fishes (e.g., chimaeras and rays) modern sharks show a very conservative body plan and a cartilaginous internal skeleton that rarely fossilizes. Complete and articulated skeletal remains of cartilaginous fishes are very rare and only a few exceptional fossiliferous Konservat-Lagerstätten yielded well-preserved fossils (Brito and Dutheil, 2004; Carvalho et al., 2004; Hovestadt et al., 2010; Marramà et al., 2017, 2023). Most of the fossil record is instead represented by isolated teeth only, which are found worldwide in marine, brackish, and freshwater sediments. These isolated teeth are often among the most common fossils available, due to a higher fossilization potential because of their structure and composition. This huge availability in the record is also explained by the fact that each shark has multiple teeth arranged in several rows and these teeth are lost and replaced many times in the biological life cycle (Budker and Whitehead, 1971).

The abundance of isolated fossil shark teeth in the palaeontological record has led in recent years to an increasing number of identified taxa (e.g., Cappetta, 2012), but the systematics, overall morphology, body size, and palaeoecology of extinct sharks are often difficult to interpret without complete and articulate skeletons. Qualitative taxonomic identification is widely used but it often leads to several discussions about the validity of the results, because of the common occurrence of teeth exhibiting remarkable morphological similarities due, for example, to evolutionary convergence (Cappetta, 1987, 2012). As valid support to taxonomic identification, some techniques based on quantitative approaches such as geometric morphometrics and traditional morphometrics are getting more and more commonly used, since they can detect even minimal morphological differences that are often difficult to observe. Some recent studies have used geometric morphometrics to validate the qualitative taxonomic identification of different genera of extinct sharks using isolated fossil teeth (e.g., Nyberg et al., 2006; Whitenack and Gottfried, 2010), while the use of traditional morphometrics has been more neglected, although Marramà and Kriwet (2017) demonstrated that it can represent a valid support for a priori qualitative identification.

This paper aims to determine whether geometric and traditional morphometrics are equally reliable for taxonomic identification when applied to the same sample. For this purpose, we consider the same sample analyzed by Marramà and Kriwet (2017), who used the traditional morphometric approach to support the taxonomic identification of 172 isolated lamniform shark teeth belonging to four different fossil and extant genera (*Brachycarcharias*, *Carcharias*, *Carcharomodus*, and *Lamna*). In this study we use, instead, geometric morphometrics on the same sample in order to: 1) validate the qualitative taxonomic separation at genus level made a priori; 2) compare the results of the two different approaches to detect whether geometric morphometrics and traditional morphometrics, when applied on the same specimens, are equally reliable in supporting the qualitative taxonomic identification in the same way or not; and 3) recognize which one of the two approaches is more effective in detecting even minimal differences and most of the morphological variation.

## MATERIALS AND METHODS

### Taxon Sampling

This study is based on the same sample used in the traditional morphometric analysis made by Marramà and Kriwet (2017), who analyzed a total of 172 isolated lamniform shark teeth, both fossil and extant, belonging to four different genera (*Brachycarcharias*, *Carcharias*, *Carcharomodus*, and *Lamna*). The choice of using different but morphologically similar genera of lamniform sharks allows to better test the capability of geometric and traditional morphometrics to detect minimal differences in shape that can be difficult to recognize only through the observation of qualitative features. Because geometric morphometrics requires consistent landmarks, incomplete specimens from the original sample used in Marramà and Kriwet (2017) were here excluded, as missing data would prevent reliable statistical comparisons (see e.g., Adams et al., 2004). Among the possible solutions for dealing with partially preserved specimens (see e.g., Gunz et al., 2005; Mitteroecker and Gunz, 2009) we chose to select a subset of the main sample that includes only the most complete specimens.

The 120 specimens used here include 40 isolated teeth from fossil species and 80 from extant species. The 40 fossil specimens come from five extinct species (*Brachycarcharias lerichei*, *Carcharias acutissima*, *C. cuspidata*, *C. gustrowensis*, and *Carcharomodus escheri*; 18, 5, 8, 1, and 8 specimens, respectively), whereas the remaining 80 specimens are from complete tooth series of two extant species: the porbeagle shark *Lamna nasus* and the sand tiger shark *Carcharias taurus* (55 and 25 specimens, respectively). Further details on provenance and age are included in Appendix 1. All the fossil teeth in the sample considered herein have been previously classified a priori using qualitative characters (Cappetta and Nolf, 2005; Cappetta, 2012; Kriwet et al., 2015; Marramà et al., 2018, 2019).

The teeth of extant taxa belong to three complete tooth series of juvenile and adult sharks. All the 25 teeth of *Carcharias taurus* are from a single juvenile individual, whereas the 55 teeth of *Lamna nasus* are from an adult (26 specimens) and a juvenile (29 specimens) individual. These two living species are used as control taxa for a better comparison between the four genera.

Since the main goal is to compare our results with those of Marramà and Kriwet (2017) the analyses were necessarily performed at the genus level,

following the methods and reasons already mentioned by the authors. For the same reason, the materials from *Carcharias taurus*, *C. acutissima*, *C. cuspidata*, and *C. gustrowensis* are grouped together, thus increasing the overall sample referable to this genus.

### Geometric Morphometrics Protocols

Geometric morphometrics is a powerful tool for the study of the morphological variation between biological forms thanks to a landmark-based approach that allows us to represent the overall body shape of an object (e.g., teeth, in this case) (Rohlf and Marcus, 1993; Zelditch et al., 2004). A total of seven homologous landmarks and eight semilandmarks were digitized using the software package TPSdig 2.32 (Rohlf, 2005) on each specimen following the scheme in Figure 1A. As illustrated in Figure 1A, all the landmarks were placed in homologous positions to cover adequately the overall shape. The eight equidistant semilandmarks were placed along the curved profile of the ventral margin of the tooth root where no homologous points can be detected. Landmarks and semilandmarks were digitized on the lingual or labial side of the tooth (since they are the only accessible sides for the fossil specimens still embedded in the sediment). Despite we analyzed a smaller subset of specimens than to the original sample of Marramà and Kriwet (2017), the use of landmarks and semilandmarks allows to obtain a larger amount of information than that provided from the traditional morphometric approach using biometric characters (i.e., measurements; see Figure 1B) (Zelditch et al., 2004).

To achieve a more reliable analysis and a better interpretation of the position of landmarks and semilandmarks by the software, all the images representing the 120 specimens considered were oriented (flipped) in the same way. Each tooth was so disposed with its basal portion facing downwards and its apical portion facing upwards, with the mesial side on the right and the distal side on the left (Figure 1A).

All the landmarks and semilandmarks coordinates were scaled, translated, and rotated using a Generalized Procrustes Analysis (GPA) to minimize the differences in size, position, and orientation in the various landmark configurations of the 120 specimens (Zelditch et al., 2004). Sliding was also done on the semilandmarks to adjust their positions on curved surfaces and to reduce non-shape variation. The GPA was performed through the software package TPSrelw 1.75 (Rohlf, 2003).

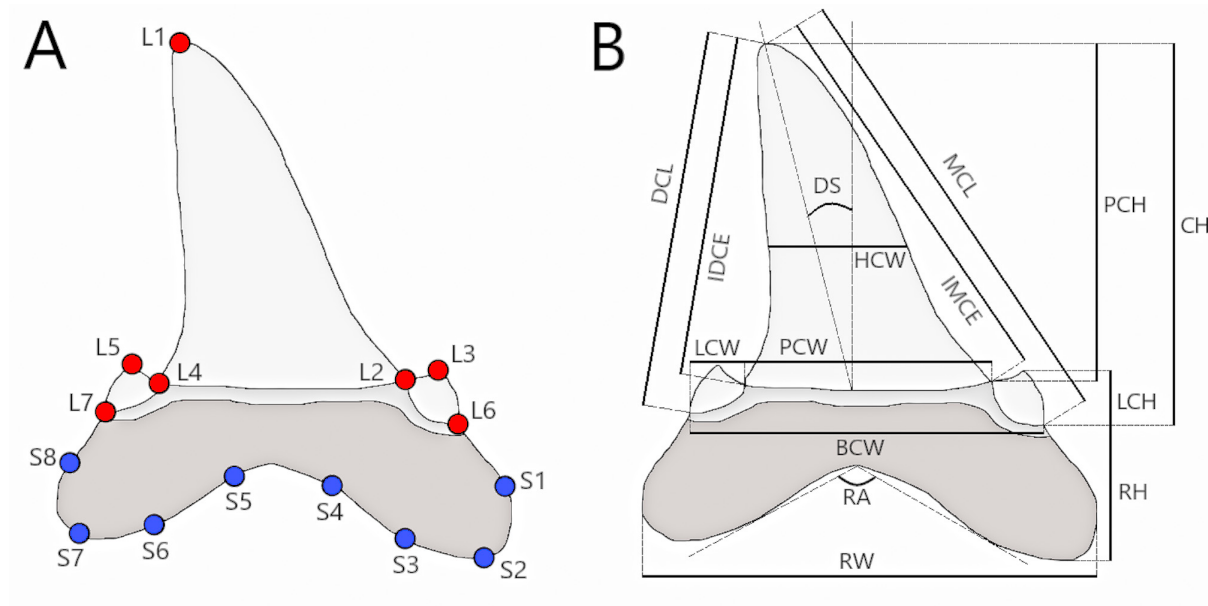


**FIGURE 1.** Geometric morphometric and traditional morphometric approaches applied to the same sample. **A**, Arrangement of landmarks (red) and semilandmarks (blue) used in this paper for each of the 120 specimens: L1, apex of the principal cusp; L2, intersection between the principal cusp and the lateral cusplet (on mesial side); L3, apex of the mesial lateral cusplet; L4, intersection between the principal cusp and the lateral cusplet (on distal side); L5, apex of the distal lateral cusplet; L6, intersection between the mesial lateral cusplet and the root; L7, intersection between the distal lateral cusplet and the root. The accurate positions of semilandmarks (S1–S8) are not defined. **B**, Terminology of the linear measurements and angles used in Marramà and Kriwet (2017) for traditional morphometrics: BCW, basal crown width; CH, crown height; DCL, distal crown edge length; DS, degree of slant; HCW, half-crown width; IDCE, inner distal crown edge length; IMCE, inner mesial crown edge length; LCH, height of lateral cusplets; LCW, width of lateral cusplets; MCL, mesial crown edge length; PCH, height of principal cusp; PCW, width of principal cusp; RA, angle between root lobes; RH, root height; RW, root width.

The new coordinates obtained from the GPA, called Procrustes coordinates, were analyzed through a Principal Component Analysis (PCA) using TPSrelw 1.75 (Rohlf, 2003). The configurations of these new coordinates are displayed in a two-dimensional graph called morphospace, which allows the visualization of the spatial distribution and separation of the 120 specimens in relation to their different shapes (Janžekovič and Novak, 2012). The morphospace is defined by the Principal Component (PCs) or Relative Warp (RWs) axes, arranged orthogonally to each other, which are vectors describing the maximum variation of specimen shape compared to the consensus configuration (mean shape) (Hotelling, 1933; James and McCulloch, 1990; Legendre and Legendre, 1998; Harper, 1999; Robertson et al., 2001; Gotelli and Ellison, 2004; Hammer and Harper, 2006; Janžekovič and Novak, 2012). Generally, more PC (or RW) axes are identified, but only those explaining more than 5% of the total variance are considered (Zelditch et al., 2004; Janžekovič and Novak, 2012). To obtain a clear visualization of the overall

sample in the morphospace, the 120 specimens are grouped together according to their genus, with the identification of four different groups (one for each genus) defined by a convex hull, the smallest convex polygon that contains all the specimens belonging to the same genera (Cornwell et al., 2006). Changes in shapes along the PC axes are visualized through deformation grid plots (see Figures 2A–B, 3–5) which are useful to understand which are the morphological traits that change the most and to identify the variables associated to each axis (see Table 1).

Fifteen measurements of the tooth morphology and related terminology used in Marramà and Kriwet (2017) are considered here (Figure 1B): basal crown width (BCW), crown height (CH), distal crown edge length (DCL), degree of slant (DS), half-crown width (HCW), inner distal crown edge length (IDCE), inner mesial crown edge length (IMCE), height of lateral cusplets (LCH), width of lateral cusplets (LCW), mesial crown edge length (MCL), height of principal cusp (PCH), width of principal cusp (PCW), angle between root lobes (RA), and root width (RW).

**TABLE 1.** Principal component axes, singular values, percent variation, cumulative percentage and associated variables for the entire sample of 120 lamniform shark teeth. To better compare the two approaches, the associated variables detected in Marramà and Kriwet (2017) are also reported. Only the first three axes (in bold) are considered for this analysis. The asterisk (\*) indicates those variables that were not considered significantly correlated to the same axis in Marramà and Kriwet (2017) (i.e.,  $|loading| \leq 0.5$ ).

PC	SV	% Variance	Cumulative %	Associated variables detected through geometric morphometrics	Associated variables detected in Marramà and Kriwet (2017) through traditional morphometrics
1	<b>1.13973</b>	<b>50.42%</b>	<b>50.42%</b>	<b>BCW, DS, HCW*, LCW*, PCH*, PCW, RA, RH*, RW</b>	<b>BCW, DS, PCW, RA, RW</b>
2	<b>0.56078</b>	<b>12.21%</b>	<b>62.62%</b>	<b>BCW, LCH, LCW, PCH*, RA, RH*, RW</b>	<b>BCW, LCH, LCW, RA, RW</b>
3	<b>0.55516</b>	<b>11.96%</b>	<b>74.59%</b>	<b>CH, DCL, DS*, HCW, IDCE*, IMCE, MCL, RH</b>	<b>CH, DCL, HCW, IMCE, MCL, RH</b>
4	0.48118	8.99%	83.58%		
5	0.35182	4.80%	88.38%		
6	0.28161	3.08%	91.45%		
7	0.25149	2.45%	93.91%		
8	0.17997	1.26%	95.17%		
9	0.17442	1.18%	96.35%		
10	0.15596	0.94%	97.29%		
11	0.13397	0.70%	97.99%		
12	0.11575	0.52%	98.51%		
13	0.10176	0.40%	98.91%		
14	0.09143	0.32%	99.23%		
15	0.07999	0.25%	99.48%		
16	0.06671	0.17%	99.65%		
17	0.05771	0.13%	99.78%		
18	0.05269	0.11%	99.89%		
19	0.03199	0.04%	99.93%		
20	0.02449	0.02%	99.95%		
21	0.01884	0.01%	99.97%		
22	0.01670	0.01%	99.98%		
23	0.01539	0.01%	99.99%		
24	0.01186	0.01%	99.99%		
25	0.00963	0.00%	100.00%		
26	0.00744	0.00%	100.00%		

(RA), root height (RH), and root width (RW). Although geometric morphometrics cannot directly link the morphological variable(s) associated to each axis (contrary to the PCA's loading values (LV), that describe how much each variable contributes to a particular principal component), we used these measurements to more easily define the morphological traits associated to the PC axes of the geometric morphometrics. Due to the transformation of multiple variables into a set of orthogonal axes made by PCA (Hotelling, 1933), more variables are usually associated simultaneously to

the same axis (see Table 1). The PCA's loading values are very useful to identify to which degree each variable is associated to each PC axis. A common rule of thumb is to consider variables with  $|loading| > 0.5$  as significant contributors to the PCs (e.g., Jolliffe, 2002; Abdi and Williams, 2010). In order to detect which one of the two approaches (traditional and geometric morphometrics) is the most effective to detect distinctiveness between groups, we compared the PCA's loading values that most contributes to shape variation in the traditional morphometrics with the Sum of Squares val-

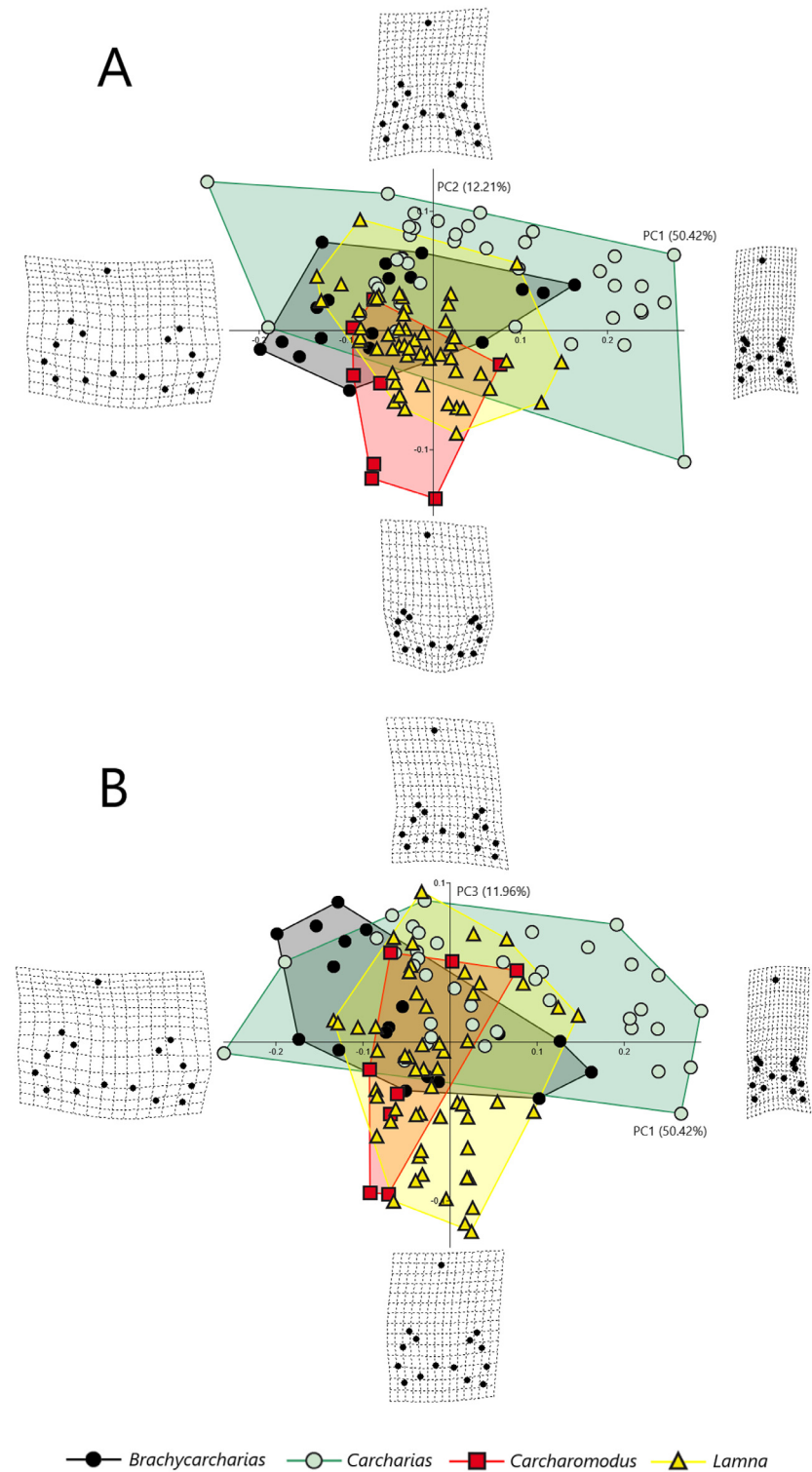


**FIGURE 2.** Morphospaces plotted on the first three PC axes considered in this study and representing the spatial distribution of the 120 specimens in the sample. The distribution of the specimens and relative convex hulls are different in each of the two morphospaces, due to the use of distinct axes, although PC1 is always plotted on abscissas. Deformation grid plots are placed at the extreme negative and positive scores of each axis. **A**, Morphospace plotted on PC1 and PC2. **B**, Morphospace plotted on PC1 and PC3.

ues (SS) from the geometric morphometric approach, i.e., the sum of squared deviations of a landmark's coordinates from the mean shape along each relative warp axis. Similarly to the loading values, the Sum of Squares values quantify the relative contribution of each landmark and semi-landmark to the deformation along the relative warps (Rohlf, 1993). Higher SS values are linked to a more significant role in shape variation along a given relative warp axis.

### Patterns of Morphospace Occupation

To assess significant differences in morphospace occupation among the four tooth groups and to evaluate if the visual separation of convex hulls in the morphospace is significantly related to differences in morphology (and taxonomy), we used two non-parametric statistical tests: PERMANOVA and ANOSIM (Table 2). The choice to use non-parametric tests is due to the incompleteness of the palaeontological data, which does not allow us to apply parametric tests (e.g., ANOVA and Chi-square) since they require a Gaussian (normal)

distribution, more easily achieved when dealing with larger sets that are hard to obtain in palaeontological analyses (Marramà et al., 2016). PERMANOVA (permutational multivariate analysis of variance) is applied to test the presence of significant differences between the distances of two or more group centroids (Anderson, 2001). The null hypothesis for PERMANOVA is that the groups have the same group centroid (Anderson, 2001). ANOSIM (analysis of similarities) is used, instead, to quantitatively define the degree of overlap between two or more groups, through calculation of an *R* function ranging from 0 (groups are indistinguishable and so completely overlapped) to 1 (groups are completely separated and so clearly different) (Clarke, 1993). The null hypothesis for ANOSIM is that the groups are completely overlapped and therefore indistinguishable (Clarke, 1993). For both tests, Euclidean distances were chosen as distance measure. A randomization with 9999 replicates is applied. The level of reliability of the results, defining the minimum probability that

**TABLE 2.** Results of the non-parametric PERMANOVA and ANOSIM tests for all the possible pairwise comparisons between the four genera on the overall sample of 120 specimens. Euclidean distances are chosen as a measure unit. The asterisks (\*) indicate significant comparisons ( $p < 0.05$ ) thereby suggesting that groups exhibit considerably different morphospace occupations.

<b>PERMANOVA</b>				
<b>p-values</b>	<i>Brachycarcharias</i>	<i>Carcharias</i>	<i>Carcharomodus</i>	<i>Lamna</i>
<i>Brachycarcharias</i>		0.0011*	0.0482*	0.0005*
<i>Carcharias</i>			0.0017*	0.0001*
<i>Carcharomodus</i>				0.0013*
<i>Lamna</i>				
<b>F-values</b>				
<i>Brachycarcharias</i>		8.975	2.844	6.913
<i>Carcharias</i>			8.573	18.92
<i>Carcharomodus</i>				5.345
<i>Lamna</i>				
<b>ANOSIM</b>				
<b>p-values</b>	<i>Brachycarcharias</i>	<i>Carcharias</i>	<i>Carcharomodus</i>	<i>Lamna</i>
<i>Brachycarcharias</i>		0.0136*	0.0474*	0.0001*
<i>Carcharias</i>			0.0034*	0.0001*
<i>Carcharomodus</i>				0.0005*
<i>Lamna</i>				
<b>R-values</b>				
<i>Brachycarcharias</i>		0.1360	0.1784	0.3448
<i>Carcharias</i>			0.3212	0.4095
<i>Carcharomodus</i>				0.3658
<i>Lamna</i>				

the null hypothesis for PERMANOVA and ANOSIM is true, is set at 0.05.

Non-parametric tests were performed using the software package PAST 5 (PAleontological STatistics) (Hammer et al., 2001).

## RESULTS

### RW Analysis on the Overall Sample

As shown in Table 1, the PCA performed on the new Procrustean coordinates of the entire sample of 120 specimens belonging to four genera (*Brachycarcharias*, *Carcharias*, *Carcharomodus*, and *Lamna*) detected a total of 26 PC axes, with only the first four (PC1, PC2, PC3, and PC4) explaining more than 5% of variation and accounting together for 83.58% of the overall sample variability. As the goal of this paper is to obtain a direct comparison between the two different approaches, only the first three axes are here illustrated and considered, since PC4 in Marramà and Kriwet (2017) explained less than 5% of variation. Two different morphospaces are then generated, each of them built on a pair of orthogonal PC axes (Figure 2A–B). Deformation grid plots illustrated represent the extreme shapes lying on lowest negative and highest positive scores of each axis.

PC1 (50.42% of total variance) explains most of the variability in the sample and is mainly related to the degree of slant (DS), to the basal and half-crown width (BCW, HCW), to the variation in height and width of the principal cusp (PCH, PCW) and root (RH, RW), to the angle between root lobes (RA) and, at least in part, to the width of the lateral cusplets (LCW). Figure 2A–B illustrates that specimens with wide and short main cusps and wide angles between root lobes, which are typical traits of the posteriormost lateral teeth, lie in negative values. Positive values of PC1 are instead associated with specimens with high and narrow main cusps and roots, and narrower angles between the narrow root lobes, features typical of the anterior shark teeth.

PC2 (12.21% of total variance) is mainly related to the height and width of the lateral cusplets (LCH, LCW), to the basal crown width (BCW), to the width and height of the root (RW, RH), to the angle between its lobes (RA) and, partially, to the height of the principal cusp (PCH). As shown in Figure 2A, negative scores of PC2 are occupied by specimens characterized by very short lateral cusplets and rounded and short root lobes, typical features of *Carcharomodus* teeth. Conversely, positive values of PC2 are related to teeth with

higher lateral cusplets, and narrow and sharp root lobes (e.g., lateral teeth of *Carcharias*).

Finally, PC3 (11.96% of total variance) is mainly related to the degree of slant of the main cusp (DS) that involves also the distal and mesial crown edge lengths (DCL, IDCE, MCL, and IMCE), but is also related, to a lesser degree, to the shape of the root lobes (defined by RW, RH, and RA), to the crown height (CH), and to the half-crown width (HCW). In Figure 2B, negative values of PC3 are occupied by specimens with weak inclinations of the main cusp and thick root lobes, whereas positive scores are related to strong inclinations of the main cusp and narrow root lobes.

The visual separation of the four taxa in the morphospaces (Figure 2A–B) is clearly supported by the results of the non-parametric tests PERMANOVA and ANOSIM for all the possible pairwise comparisons (Table 2). Both PERMANOVA and ANOSIM clearly support the analysis through geometric morphometrics, underlining the different morphospace occupation of the genera, and so suggesting that this approach is useful to separate taxa. PERMANOVA rejects the null hypothesis of equal group centroids, demonstrating that group centroids are significantly distant from each other ( $p = 0.0001$ ;  $F = 10.37$ ). Also, ANOSIM rejects its null hypothesis, showing that the groups, although overlapped in some portions of the morphospace, are still clearly different ( $p = 0.0001$ ;  $R = 0.3427$ ).

### RW Analyses on the Pairwise Comparisons

In order to maximize the separation between the four genera, new RW analyses were performed and new morphospaces were generated for the pairwise comparisons reported in Table 2. Following Marramà and Kriwet (2017), only comparisons involving *Brachycarcharias* with the other three taxa are considered herein, since the goal of that paper was to solve contradicting taxonomic issues related to this taxon. As in Marramà and Kriwet (2017), the three morphospaces of the pairwise comparisons are built only on the first two RW axes explaining most of morphological variation. Non-parametric tests (PERMANOVA and ANOSIM) were also performed for each of the three pairwise comparisons.

***Brachycarcharias* vs *Lamna*.** As shown in Table 3, a total of 26 PC axes are identified by the RW analysis for the comparison between *Brachycarcharias* and *Lamna*, with the first five explaining more than 5% of variation. PC1 (37.33% of total variation) is related to the variation in height and width of the principal cusp, lateral cusplets, and root and

**TABLE 3.** Principal component axes, singular values, percent variation, cumulative percentage and associated variables for the sample of *Brachycarcharias* and *Lamna*. Only the first two axes (in bold) are considered. The asterisk (\*) indicates those variables that were not considered significantly correlated to the same axis in Marramà and Kriwet (2017) (i.e.,  $|loading| \leq 0.5$ ).

PC	SV	% Variance	Cumulative %	Associated variables detected through geometric morphometrics	Associated variables detected in Marramà and Kriwet (2017) through traditional morphometrics
1	<b>0.64781</b>	<b>37.33%</b>	<b>37.33%</b>	BCW*, DS, HCW, LCH*, LCW*, PCH*, PCW*, RA*, RH*, RW*	DS, HCW, IMCE, MCL
2	<b>0.45347</b>	<b>18.29%</b>	<b>55.62%</b>	DS*, RA*, RH*, RW*	BCW, LCH, LCW, MCL
3	0.38620	13.27%	68.89%		
4	0.31342	8.74%	77.63%		
5	0.29320	7.65%	85.27%		
6	0.22793	4.62%	89.90%		
7	0.17298	2.66%	92.56%		
8	0.14481	1.87%	94.42%		
9	0.12003	1.28%	95.70%		
10	0.10939	1.06%	96.77%		
11	0.09999	0.89%	97.66%		
12	0.08568	0.65%	98.31%		
13	0.07123	0.45%	98.76%		
14	0.06663	0.39%	99.16%		
15	0.05813	0.30%	99.46%		
16	0.04545	0.18%	99.64%		
17	0.04265	0.16%	99.80%		
18	0.03261	0.09%	99.90%		
19	0.02009	0.04%	99.93%		
20	0.01641	0.02%	99.96%		
21	0.01208	0.01%	99.97%		
22	0.01110	0.01%	99.98%		
23	0.00939	0.01%	99.99%		
24	0.00784	0.01%	100.00%		
25	0.00533	0.00%	100.00%		
26	0.00460	0.00%	100.00%		

to the degree of slant, whereas PC2 (18.29%) is related to the degree of slant and to root shape. As illustrated in Figure 3, despite a certain amount of overlap in the central portion of the morphospace, these two taxa are clearly separated along PC1 and PC2. *Brachycarcharias* occupies more extensively both the extreme negative and positive values of PC1. Despite a more complete sample of *Lamna* teeth, extreme negative scores are only occupied by *Brachycarcharias* teeth characterized by wider roots, main cusps, and lateral cusplets. Also, a certain portion of the morphospace on positive scores is only occupied by *Brachycarcharias* teeth having narrower and higher roots, main

cusps, and lateral cusplets. Conversely, the *Lamna* convex hull appears to be more extended along the extreme negative and positive scores of PC2. Specifically, negative values indicate specimens with smaller root lobes, whereas positive PC2 values are linked to stouter, higher, and massive roots. The visual separation of the two groups in the morphospace is clearly supported in Table 4 by the non-parametric tests PERMANOVA ( $p = 0.0001$ ) and ANOSIM ( $p = 0.0001$ ).

***Brachycarcharias* vs *Carcharias*.** According to Table 5, the RW analysis performed for the comparison between *Brachycarcharias* and *Carcha-*

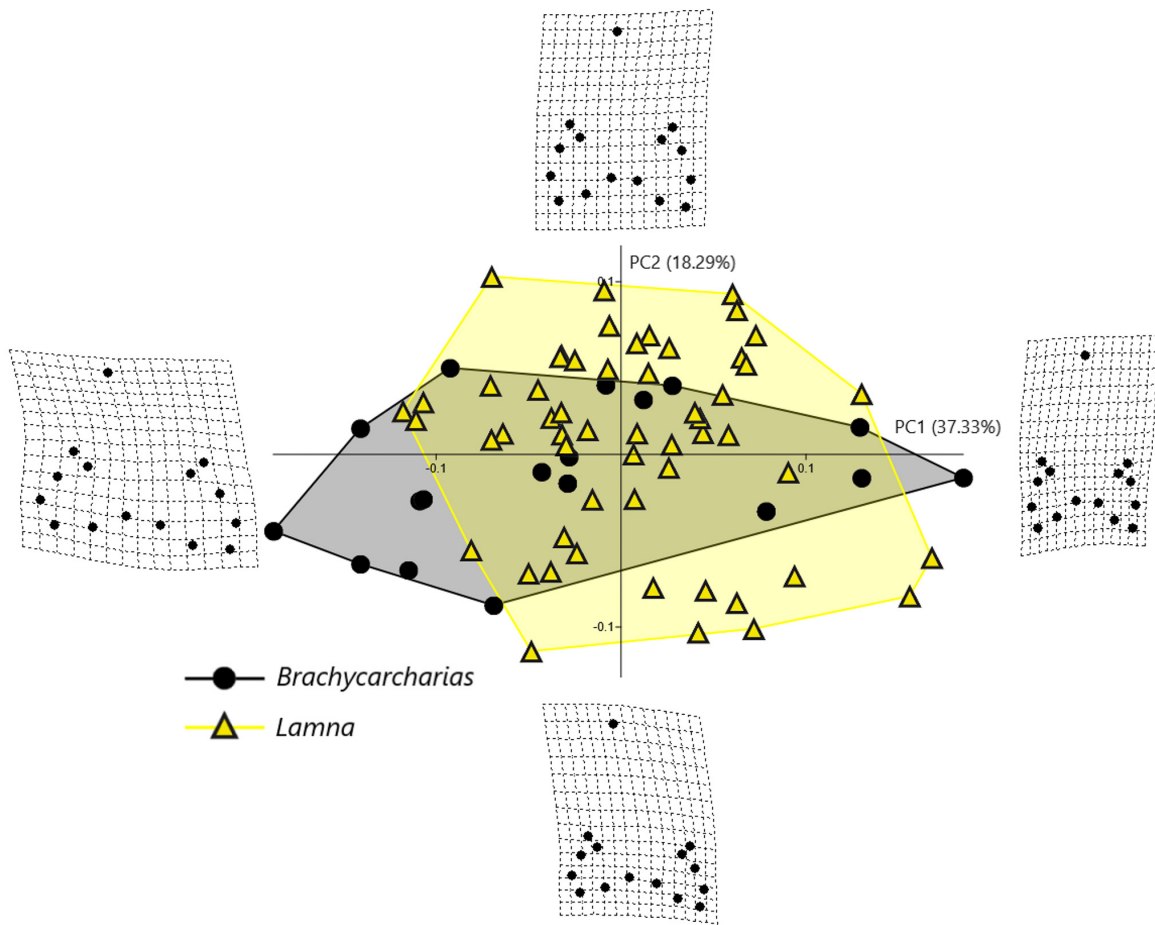


**FIGURE 3.** Morphospace plotted on PC1 and PC2 showing the spatial distribution of *Brachycarcharias* and *Lamna* teeth.

**TABLE 4.** Results of the non-parametric PERMANOVA and ANOSIM tests for the comparison between *Brachycarcharias* and *Lamna* morphospaces.

<b>PERMANOVA</b>		
<b>p-values</b>	<i>Brachycarcharias</i>	<i>Lamna</i>
<i>Brachycarcharias</i>		0.0001*
<i>Lamna</i>		
<b>F-values</b>		
<i>Brachycarcharias</i>		7.619
<i>Lamna</i>		
<b>ANOSIM</b>		
<b>p-values</b>	<i>Brachycarcharias</i>	<i>Lamna</i>
<i>Brachycarcharias</i>		0.0001*
<i>Lamna</i>		
<b>R-values</b>		
<i>Brachycarcharias</i>		0.3497
<i>Lamna</i>		

*rias* detected a total of 26 axes, with only the first three explaining more than 5% of variation. PC1 (73.11%) and PC2 (8.30%) are roughly related to the same morphological variation detected for the first pairwise comparison (*Brachycarcharias* vs *Lamna*) with the two morphospaces that, although a certain degree of overlap, occupy different portions of the plane. In particular, Figure 4 reveals that *Carcharias* occupies the extreme positive and negative scores of the PC1 not occupied by *Brachycarcharias*, suggesting that the living genus possesses teeth with more narrow and high main cusps and with longer and narrower root lobes, whereas this latter occupies part of the quadrant defined by negative scores of PC1 and positive scores of PC2, not occupied by *Carcharias*, likely related to the presence of teeth with very wide roots and big lateral cuspules. Also, for this comparison, the separation and overlapping of the two groups in the morphospace are significantly sup-

**TABLE 5.** Principal component axes, singular values, percent variation, cumulative percentage and associated variables for the sample of *Brachycarcharias* and *Carcharias*. Only the first two axes (in bold) are considered. The asterisk (\*) indicates those variables that were not considered significantly correlated to the same axis in Marramà and Kriwet (2017) (i.e.,  $|loading| \leq 0.5$ ).

PC	SV	% Variance	Cumulative %	Associated variables detected through geometric morphometrics	Associated variables detected in Marramà and Kriwet (2017) through traditional morphometrics
1	<b>1.03990</b>	73.11%	73.11%	BCW, DS, HCW, LCH, LCW, PCH*, PCW, RA, RH*, RW	BCW, DS, HCW, IDCE, LCH, LCW, PCW, RA, RW
2	<b>0.35049</b>	8.30%	81.41%	DS*, RA*, RH*, RW*	BCW, LCH, LCW
3	0.28140	5.35%	86.76%		
4	0.24456	4.04%	90.81%		
5	0.19215	2.50%	93.30%		
6	0.15544	1.63%	94.94%		
7	0.14789	1.48%	96.42%		
8	0.10375	0.73%	97.14%		
9	0.09766	0.64%	97.79%		
10	0.09036	0.55%	98.34%		
11	0.07910	0.42%	98.76%		
12	0.06824	0.31%	99.08%		
13	0.06346	0.27%	99.35%		
14	0.05448	0.20%	99.55%		
15	0.04376	0.13%	99.68%		
16	0.04071	0.11%	99.79%		
17	0.03572	0.09%	99.88%		
18	0.02989	0.06%	99.94%		
19	0.01863	0.02%	99.96%		
20	0.01303	0.01%	99.97%		
21	0.01201	0.01%	99.98%		
22	0.00997	0.01%	99.99%		
23	0.00767	0.00%	99.99%		
24	0.00692	0.00%	100.00%		
25	0.00503	0.00%	100.00%		
26	0.00332	0.00%	100.00%		

ported by the results obtained from PERMANOVA ( $p = 0.0010$ ) and ANOSIM ( $p = 0.0059$ ) in Table 6.

***Brachycarcharias* vs *Carcharomodus*.** According to Table 7, of the 25 axes identified by the RW analysis for the pairwise comparison between *Brachycarcharias* and *Carcharomodus*, only the first five explain more than 5% of variation. PC1 (48.38%) is always related to the variation in height and width of the principal cusp, lateral cusplets and root and to the degree of slant, resembling the morphological variation associated to the same PC axis in the two previous pairwise comparisons (*Brachycarcharias* vs *Lamna* and *Brachycarcharias* vs *Carcharias*). PC2 (18.17%), on the other hand,

appears mostly related to the heights and widths of lateral cusplets. As reported in Figure 5, despite the little overlap of the convex hulls in the central portion of the morphospace, these two genera are clearly distinguishable and separate from each other along both PC1 and PC2. *Carcharomodus* mostly occupies the positive values of PC2, associated with teeth having extremely small lateral cusplets, whereas some teeth of *Brachycarcharias* occupy more negative scores of PC2, as they have taller lateral cusplets. *Brachycarcharias* convex hull is noticeably more extended also in the extreme negative and positive values of PC1, suggesting the presence of higher disparity in tooth shapes,

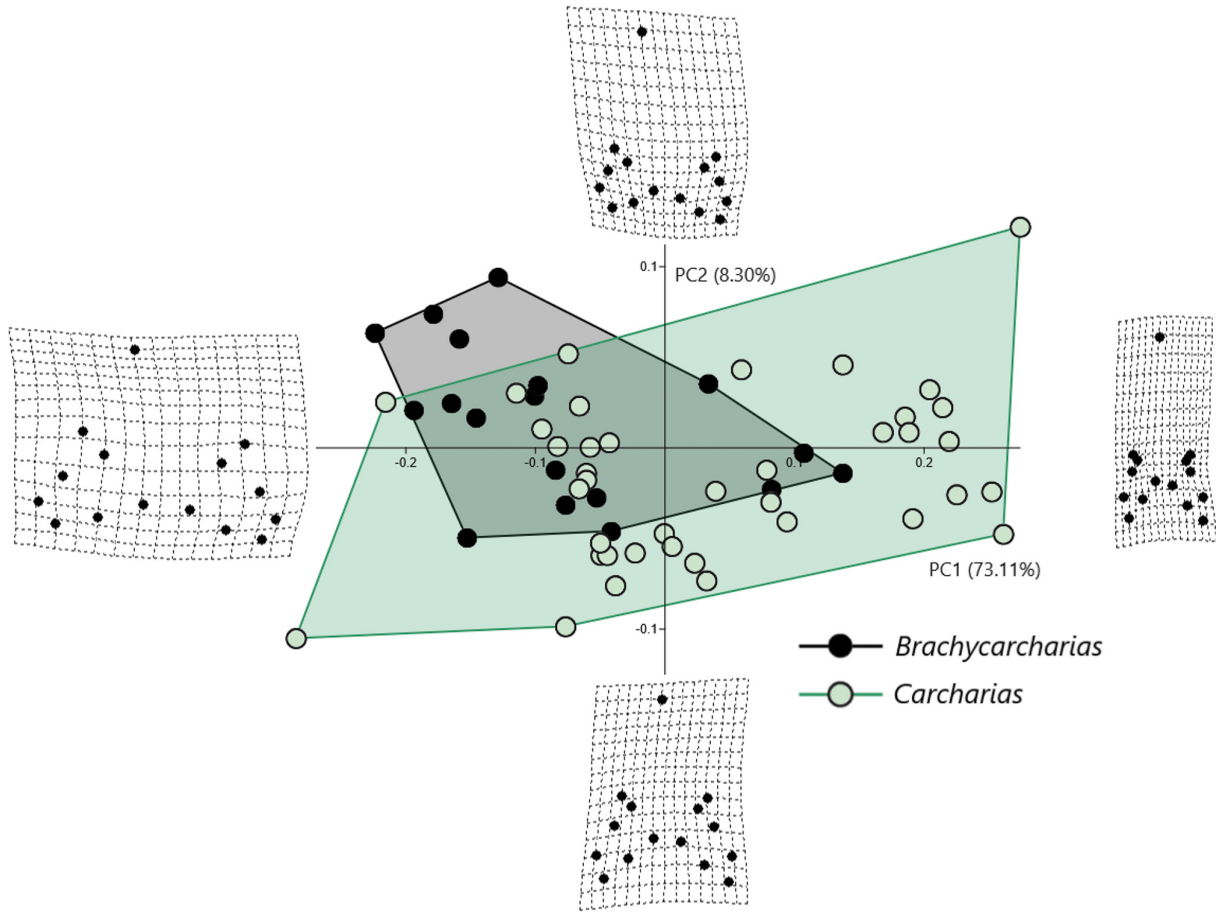


**FIGURE 4.** Morphospace plotted on PC1 and PC2 showing the spatial distribution of *Brachycarcharias* and *Carcharias* teeth.

although sampling bias due to more a reduced sample must be considered. The different morphospace occupation of these two taxa is statistically supported, also in this case, by the results of PERMANOVA ( $p = 0.0170$ ) and ANOSIM ( $p = 0.0176$ ) in Table 8.

#### Landmarks' Relative Contributions

We analyzed the Sum of Squares values (SS), i.e., the sum of squared deviations of a landmark's coordinates from the mean shape along each relative warp axis, that quantify the relative contribution of each landmark and semilandmark to the deformation along the relative warps (Rohlf, 1993), to better understand which the morphological traits that most contribute to the overall morphological disparity in the overall sample and in the pairwise comparison analyses are. Higher SS values are linked to a more significant role in shape variation along a given relative warp axis. The

**TABLE 6.** Results of the non-parametric PERMANOVA and ANOSIM tests for the comparison between *Brachycarcharias* and *Carcharias* morphospaces.

<b>PERMANOVA</b>		
<b>p-values</b>	<i>Brachycarcharias</i>	<i>Carcharias</i>
<i>Brachycarcharias</i>		0.0010*
<i>Carcharias</i>		
<b>F-values</b>		
<i>Brachycarcharias</i>		9.911
<i>Carcharias</i>		
<b>ANOSIM</b>		
<b>p-values</b>	<i>Brachycarcharias</i>	<i>Carcharias</i>
<i>Brachycarcharias</i>		0.0059*
<i>Carcharias</i>		
<b>R-values</b>	<i>Brachycarcharias</i>	<i>Carcharias</i>
<i>Brachycarcharias</i>		0.1561
<i>Carcharias</i>		

**TABLE 7.** Principal component axes, singular values, percent variation, cumulative percentage and associated variables for the sample of *Brachycarcharias* and *Carcharomodus*. Only the first two axes (in bold) are considered. The asterisk (\*) indicates those variables that were not considered significantly correlated to the same axis in Marramà and Kriwet (2017) (i.e.,  $|loading| \leq 0.5$ ).

PC	SV	% Variance	Cumulative %	Associated variables detected through geometric morphometrics	Associated variables detected in Marramà and Kriwet (2017) through traditional morphometrics
1	<b>0.47240</b>	<b>48.38%</b>	<b>48.38%</b>	<b>BCW*, DS, HCW*, LCH*, LCW*, PCH*, PCW*, RA*, RH*, RW*</b>	<b>DS, IMCE, MCL</b>
2	<b>0.28952</b>	<b>18.17%</b>	<b>66.56%</b>	<b>DS*, LCH, LCW, RA, RH*, RW*</b>	<b>HCW, LCH, LCW, RA</b>
3	0.26025	14.68%	81.24%		
4	0.16835	6.14%	87.39%		
5	0.15207	5.01%	92.40%		
6	0.10016	2.18%	94.58%		
7	0.08009	1.39%	95.97%		
8	0.06775	1.00%	96.96%		
9	0.06253	0.85%	97.81%		
10	0.05654	0.69%	98.50%		
11	0.04794	0.50%	99.00%		
12	0.04062	0.36%	99.36%		
13	0.03133	0.21%	99.57%		
14	0.02642	0.15%	99.72%		
15	0.02145	0.10%	99.82%		
16	0.01764	0.07%	99.89%		
17	0.01470	0.05%	99.94%		
18	0.01285	0.04%	99.97%		
19	0.00781	0.01%	99.99%		
20	0.00623	0.01%	99.99%		
21	0.00344	0.00%	100.00%		
22	0.00301	0.00%	100.00%		
23	0.00256	0.00%	100.00%		
24	0.00081	0.00%	100.00%		
25	0.00028	0.00%	100.00%		

seven landmarks (L1–L7) and eight semilandmarks (S1–S8) (see Figure 1A) and their SS values are provided by TPSrelw 1.75 (Rohlf, 2003) and are listed in Tables 9–12. The values are then compared to the loading values associated with the PC axes listed in Marramà and Kriwet (2017) that were used, in the same way, to interpret the “meaning” of the components that identify the main factors to which a PC axis is related in the PCA (Hammer et al., 2001). This comparison between the two values (sum of squares and loading values) from the two different approaches (geometric and traditional morphometrics) will allow us to determine which approach is more effective in

evaluating the relative ability to detect the greatest amount of morphological variation.

In the overall sample analysis shown in Table 9, the landmarks L2, L4, L6, and L7, which are associated to the width of principal cusp and to the basal crown width, contribute to most of the morphological variation, followed by the semilandmarks S4 and S5 that are related to the variation associated to the angle between root lobes. Also, in the pairwise comparisons between *Brachycarcharias* vs *Lamna* and *Brachycarcharias* vs *Carcharias*, reported respectively in Tables 10–11, the landmarks L2, L4, L6, and L7 and the semilandmarks S4 and S5 are those contributing to most of

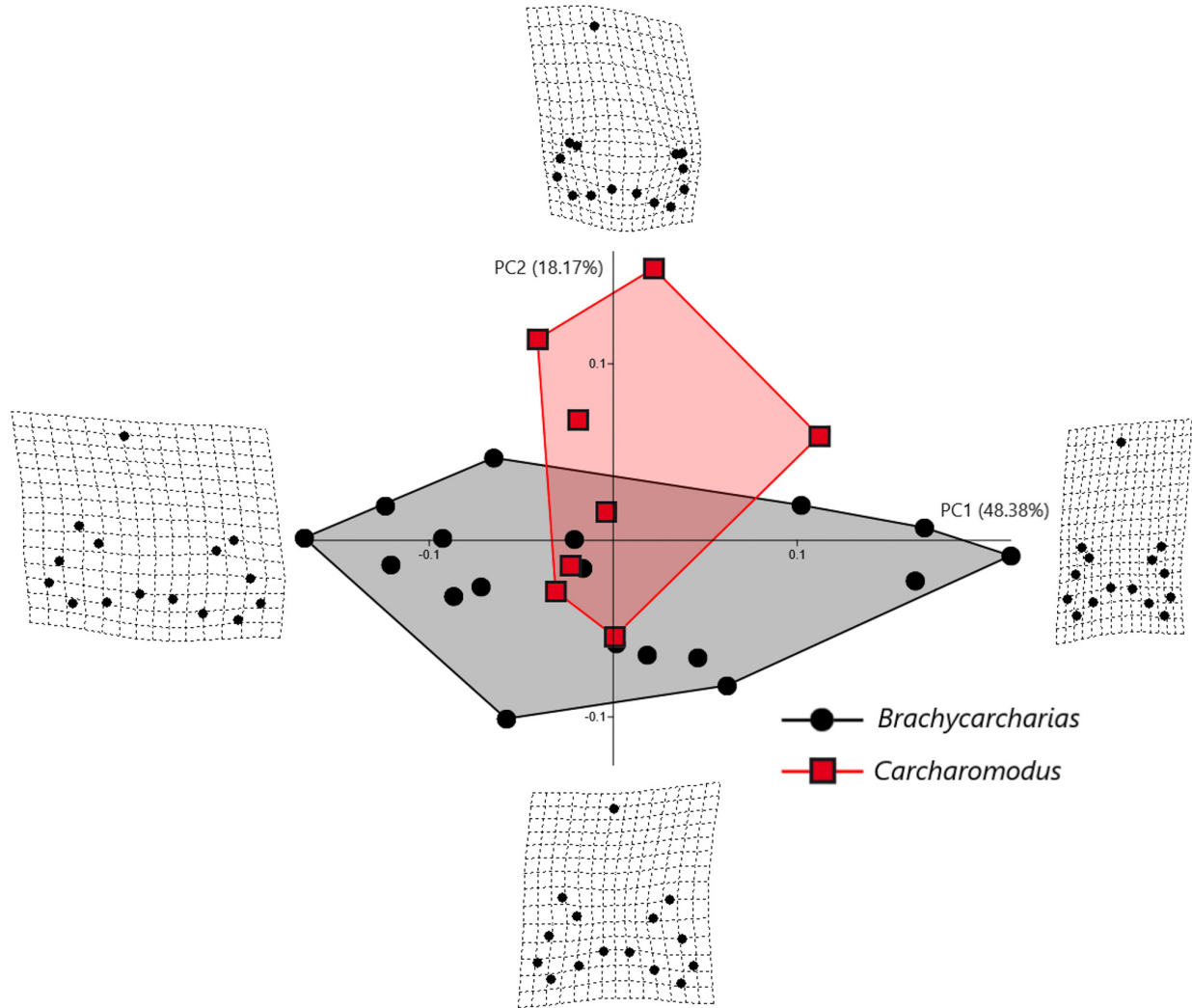


**FIGURE 5.** Morphospace plotted on PC1 and PC2 showing the spatial distribution of *Brachycarcharias* and *Carcharomodus* teeth.

the morphological variation. Conversely, in the pairwise comparison *Brachycarcharias* vs *Carcharomodus* in Table 12, the semilandmarks S1, S2, S3, S4, S5, and S6, which are associated to the root shape on the mesial side, and to the angle between lobes, mostly contribute to the shape variation.

## DISCUSSION AND CONCLUSIONS

This study aimed to assess whether traditional and geometric morphometric methods are equally valid for taxonomic identification and to recognize which approach is more effective. Our results demonstrate that geometric morphometrics is a robust and effective tool for testing and corroborating taxonomic hypotheses based on isolated fossil shark teeth, supporting previous research indicat-

ing that tooth morphology is a reliable criterion for distinguishing genera (e.g., Nyberg et al., 2006; Whitenack and Gottfried, 2010; Marramà and Kriwet, 2017).

Although some overlap in convex hulls was observed in geometric morphometric analyses, the four genera (*Brachycarcharias*, *Carcharias*, *Carcharomodus*, and *Lamna*) were clearly separated both in the overall morphospace and in pairwise comparisons (see Figures 2A–B, 3–5). These results indicate that distinct portions of the morphospace are uniquely occupied by specific taxa, reflecting meaningful morphological differentiation. In particular, the separation between *Brachycarcharias* and *Lamna* (Figure 3) corroborates the results of Marramà and Kriwet (2017) and supports earlier ecological and trophic interpretations related to these taxa (cf. Purdy and Francis, 2007;

**TABLE 8.** Results of the non-parametric PERMANOVA and ANOSIM tests for the comparison between *Brachycarcharias* and *Carcharomodus* morphospaces.

PERMANOVA		
p-values	<i>Brachycarcharias</i>	<i>Carcharomodus</i>
<i>Brachycarcharias</i>		0.0170*
<i>Carcharomodus</i>		
F-values		
<i>Brachycarcharias</i>		3.584
<i>Carcharomodus</i>		
ANOSIM		
p-values	<i>Brachycarcharias</i>	<i>Carcharomodus</i>
<i>Brachycarcharias</i>		0.0176*
<i>Carcharomodus</i>		
R-values		
<i>Brachycarcharias</i>		0.2281
<i>Carcharomodus</i>		

**TABLE 9.** Relative contribution of each landmark point measured as sum of squares in the overall sample analysis.

Landmark	Sum of squares
L2	0.13815
L4	0.11717
L6	0.08432
L7	0.08378
L3	0.07663
S4	0.07339
S5	0.06989
L5	0.06782
S1	0.06166
S8	0.06071
S6	0.04959
S3	0.04803
S7	0.03704
S2	0.03151
L1	0.00031
Sum	1.00

Maisch et al., 2014). The taxonomic separation is further supported in Table 4 by non-parametric statistical tests such as PERMANOVA and ANOSIM, which revealed significant differences in tooth morphology and morphospace occupation. The lower R-values reported in Tables 6, 8 for the *Brachycarcharias*–*Carcharias* and *Brachycarcharias*–*Carcharomodus* comparisons (Figures 4–5) still support intergeneric morphological variation. The

**TABLE 10.** Relative contribution of each landmark point measured as sum of squares in the pairwise comparison between *Brachycarcharias* and *Lamna*.

Landmark	Sum of squares
L2	0.10848
L7	0.09806
L6	0.09308
L4	0.09015
S4	0.07894
S5	0.07474
S8	0.07394
S1	0.07099
L3	0.06272
L5	0.05617
S6	0.05526
S3	0.05421
S7	0.04505
S2	0.03785
L1	0.00036
Sum	1.00

**TABLE 11.** Relative contribution of each landmark point measured as sum of squares in the pairwise comparison between *Brachycarcharias* and *Carcharias*.

Landmark	Sum of squares
L2	0.13886
L4	0.12815
S4	0.08313
L6	0.08096
S5	0.07996
L7	0.07889
L3	0.06229
S1	0.06139
L5	0.06082
S8	0.05543
S6	0.05326
S3	0.05042
S7	0.03542
S2	0.03073
L1	0.00029
Sum	1.00

consistent statistical significance ( $p < 0.05$ ) across comparisons, despite relatively low R-values that imply larger morphological overlays since the presence of similar specimens, suggests partial mor-

**TABLE 12.** Relative contribution of each landmark point measured as sum of squares in the pairwise comparison between *Brachycarcharias* and *Carcharomodus*.

Landmark	Sum of squares
S4	0.10653
S5	0.10221
S1	0.09080
S3	0.08573
S6	0.07896
S2	0.07521
L6	0.07518
L2	0.07300
L4	0.06290
S8	0.05913
L7	0.05603
S7	0.05576
L5	0.04008
L3	0.03817
L1	0.00030
Sum	1.00

phylogenetic convergence or retained ancestral traits among these lamniform genera.

Both morphometric approaches demonstrated the capacity to detect intergeneric morphological variation. However, differences in morphospace occupation and convex hull spatial extension may partly reflect sample size variation, especially the more complete and morphologically diverse representation of extant taxa (*Carcharias taurus*, *Lamna nasus*) compared to the limited fossil record of *Carcharomodus*. Nonetheless, the occupation of unique regions of morphospace by fossil taxa, not shared with extant forms, suggests that observed shape differences are biologically meaningful and not merely sampling artifacts.

Geometric morphometrics detected all shape differences identified by the traditional approach and additionally captured variables that were not statistically significant in the traditional analysis (i.e., variables with  $|loading| \leq 0.5$ ; see Jolliffe, 2002; Abdi and Williams, 2010). This increased sensitivity supports the growing consensus on the utility of the geometric morphometrics in taxonomic studies (Elewa, 2004).

Some variables were found to be associated to the same axes in both methods, but the geometric approach identified a broader set of shape contributors (Table 1). In pairwise comparisons (Tables 3, 5, 7), certain variables were exclusive to one method, likely due to methodological differences

and sample size discrepancies. Despite this, results were broadly comparable, as the 15 biometric characters (i.e., the set of 13 linear measurements and two angles) from Marramà and Kriwet (2017) closely correspond with the landmark configuration used in our study, both adequately representing the overall tooth morphology (see also Ilić et al., 2019).

In addition, landmark contribution analyses (Tables 9–12) reveal that traits such as the width of the principal cusp, the basal crown and root width and the angle between root lobes are the primary shape drivers in the overall sample, as well as in the *Brachycarcharias*–*Lamna* and *Brachycarcharias*–*Carcharias* comparisons. In contrast, root shape and the lobe angle dominate in the *Brachycarcharias*–*Carcharomodus* comparison, further highlighting shape-based distinctions among genera.

Geometric and traditional morphometric techniques are thus confirmed as powerful tools for identifying subtle morphological differences in isolated fossil shark teeth belonging to morphologically similar lamniform genera. Importantly, both approaches reliably support prior qualitative taxonomic assignments, consistently distinguishing the four genera analysed herein. While geometric morphometrics has gained increasing application due to its greater precision and visualization potential (Elewa, 2004; Zelditch et al., 2004), traditional morphometrics remains a practical alternative, particularly when working with fragmented or incomplete specimens (Marramà and Kriwet, 2017).

Geometric morphometrics has been widely used in palaeontology to mitigate issues of over-lumping or over-splitting and to identify evolutionary convergence and morphological adaptations (Friedman, 2010; Hedrick and Dodson, 2013; Frédéric et al., 2016; Marramà et al., 2016; Marramà and Carnevale, 2017). These quantitative approaches, however, are not intended to replace qualitative assessments, which remain crucial for identifying traits not readily captured numerically but might serve as tools to test the accuracy of qualitative taxonomic hypotheses (Marramà and Kriwet, 2017).

Supporting previous comparisons of geometric and traditional morphometrics on extant taxa (Maderbacher et al., 2008; Ilić et al., 2019), our study confirms that geometric morphometrics appears more effective in detecting a greater amount of morphological variation and, for this reason, it should be especially preferred in taxonomic and palaeobiological analyses of fossil shark teeth.

## ACKNOWLEDGEMENTS

We thank R. Zorzin (Museo Civico di Storia Naturale di Verona), M. Cerato (Museo dei Fossili di Bolca), M. Fornasiero (Museo di Geologia e Paleontologia dell'Università di Padova), E. Bernard (Natural History Museum, London), A. Palandacic (Naturhistorisches Museum, Vienna), S. Fütting and W. Eckloff (Museum für Natur und

Umwelt, Lübeck) for the facilities and access to fossil material under their care. The manuscript was improved with constructive review provided by Jacopo Amalfitano (Università degli Studi di Padova) and editorial comments by Zoltán Barkaszi. This work was supported by grants ex-60% 2024 from the Università degli Studi di Torino to GC.

---

## REFERENCES

- Abdi, H. and Williams, L.J. 2010. Principal component analysis. *Wires Computational Statistics*, 2(4):433–459. <https://doi.org/10.1002/wics.101>
- Adams, D.C., Rohlf, F.J., and Slice, D.E. 2004. Geometric morphometrics: ten years of progress following the “revolution”. *Italian Journal of Zoology*, 71(1):5–16. <https://doi.org/10.1080/11250000409356545>
- Anderson, M.J. 2001. A new method for non-parametric multivariate analysis of variance. *Austral Ecology*, 26(1):32–46. <https://doi.org/10.1111/j.1442-9993.2001.01070.pp.x>
- Brito, P.M. and Dutheil, D.B. 2004. A preliminary systematic analysis of Cretaceous guitarfishes from Lebanon, p. 101–109. In Arratia, G. and Tintori, A. (eds.), *Mesozoic Fishes 3 — Systematics, Paleoenvironments and Biodiversity*. Verlag Dr. Friedrich Pfeil, München, Germany.
- Budker, P. and Whitehead, P.J.P. 1971. *The Life of Sharks*. Weidenfeld & Nicolson, London.
- Cappetta, H. 1987. Chondrichthyes II — Mesozoic and Cenozoic Elasmobranchii. In series: Schultze, H.P. (ed.), *Handbook of Paleoichthyology*, Volume 3B. Verlag Dr. Friedrich Pfeil, München, Germany.
- Cappetta, H. 2012. Chondrichthyes V — Mesozoic and Cenozoic Elasmobranchii: Teeth. In series: Schultze, H.P. (ed.), *Handbook of Paleoichthyology*, Volume 3E. Verlag Dr. Friedrich Pfeil, München, Germany.
- Cappetta, H. and Nolf, D. 2005. Revision of some Odontaspidae (Neoselachii: Lamniformes) from the Paleocene and Eocene of the North Sea Basin. *Bulletin de l'Institut Royal des Sciences Naturelles de Belgique, Sciences de la Terre*, 75:237–266.
- Carvalho, M.R. de., Maisey, J.G., and Grande, L. 2004. Freshwater stingrays of the Green River Formation of Wyoming (Early Eocene), with the description of a new genus and species and an analysis of its phylogenetic relationships (Chondrichthyes: Myliobatiformes). *Bulletin of the American Museum of Natural History*, 284:1–136. [https://doi.org/10.1206/0003-0090\(2004\)284%3C0001:fsotgr%3E2.0.co;2](https://doi.org/10.1206/0003-0090(2004)284%3C0001:fsotgr%3E2.0.co;2)
- Clarke, K.R. 1993. Non-parametric multivariate analysis of changes in community structure. *Australian Journal of Ecology*, 18(1):117–143. <https://doi.org/10.1111/j.1442-9993.1993.tb00438.x>
- Cornwell, W.K., Schwilk, L.D.W., and Ackerly, D.D. 2006. A trait-based test for habitat filtering: convex hull volume. *Ecology*, 87(6):1465–1471. [https://doi.org/10.1890/0012-9658\(2006\)87\[1465:attfhf\]2.0.co;2](https://doi.org/10.1890/0012-9658(2006)87[1465:attfhf]2.0.co;2)
- Dulvy, N.K., Fowler, S.L., Musick, J.A., Cavanagh, R.D., Kyne, P.M., Harrison, L.R., Carlson, J.K., Davidson, L.N.K., Fordham, S.V., Francis, M.P., Pollock, C.M., Simpfendorfer, C.A., Burgess, G.H., Carpenter, K.E., Compagno, L.J.V., Ebert, D.A., Gibson, C., Heupel, M.R., Livingstone, S.R., Sanciangco, J.C., Stevens, J.D., Valenti, S., and White, W.T. 2014. Extinction risk and conservation of the world's sharks and rays. *eLife*, 3:e00590. <https://doi.org/10.7554/eLife.00590>
- Elewa, A.M.T. 2004. *Morphometrics: Applications in Biology and Paleontology*. Springer-Verlag, Heidelberg, Germany. <https://doi.org/10.1007/978-3-662-08865-4>

- Frédéric, B., Marramà, G., Carnevale, G., and Santini, F. 2016. Non-reef environments impact the diversification of extant jacks, remoras and allies (Carangoidei, Percomorpha). *Proceedings of the Royal Society B*, 283(1842):20161556. <https://doi.org/10.1098/rspb.2016.1556>
- Friedman, M. 2010. Explosive morphological diversification of spiny-finned teleost fishes in the aftermath of the end-Cretaceous extinction. *Proceedings of the Royal Society B*, 277(1688):1675–1683. <https://doi.org/10.1098/rspb.2009.2177>
- Gotelli, N.J. and Ellison, A.M. 2004. *A Primer of Ecological Statistics*, Second Edition. Sinauer Associates, Sunderland, Massachusetts.
- Gunz, P., Mitteroecker, P., and Bookstein, F.L. 2005. Semilandmarks in three dimensions, p. 73–98. In Slice, D.E. (ed.), *Modern Morphometrics in Physical Anthropology*. Springer, Boston, Massachusetts. [https://doi.org/10.1007/0-387-27614-9\\_3](https://doi.org/10.1007/0-387-27614-9_3)
- Hammer, Ø. and Harper, D.A.T. 2006. *Paleontological Data Analysis*. Blackwell Publishing, Malden, Massachusetts. <https://doi.org/10.1002/9780470750711>
- Hammer, Ø., Harper, D.A.T., and Ryan, P.D. 2001. PAST: paleontological statistics software package for education and data analysis. *Palaeontologia Electronica*, 4(1):1–9. [https://palaeo-electronica.org/2001\\_1/past/issue1\\_01.htm](https://palaeo-electronica.org/2001_1/past/issue1_01.htm)
- Harper, D.A.T. 1999. *Numerical Palaeobiology: Computer-based Modelling and Analysis of Fossils and their Distributions*. John Wiley & Sons, Chichester. <https://doi.org/10.1017/S0016756800334410>
- Hedrick, B.P. and Dodson, P. 2013. Lujiautun psittacosaurids: understanding individual and taphonomic variation using 3D geometric morphometrics. *PLoS ONE*, 8(8):e69265. <https://doi.org/10.1371/journal.pone.0069265>
- Hotelling, H. 1933. Analysis of a complex of statistical variables into principal components. *Journal of Educational Psychology*, 24(7):498–520. <https://doi.org/10.1037/h0070888>
- Hovestadt, D.C., Hovestadt-Euler, M., and Micklich, N. 2010. A review of the chondrichthyan fauna of Grube Unterfeld (Frauenweiler) clay pit. *Kaupia*, 17:57–71.
- Ilić, M., Jović, V., Stamenković, G., Marković, V., Simić, V., Paunović, M., and Crnobrnja-Isailović, J. 2019. Geometric vs. traditional morphometric methods for exploring morphological variation of tadpoles at early developmental stages. *Amphibia-Reptilia*, 40(4):499–509. <https://doi.org/10.1163/15685381-00001193>
- James, F.C. and McCulloch, C.E. 1990. Multivariate analysis in ecology and systematics: Panacea or Pandora's box? *Annual Review of Ecology, Evolution and Systematics*, 21:129–166. <https://doi.org/10.1146/annurev.es.21.110190.001021>
- Janžekovič, F. and Novak, T. 2012. Chapter 8. PCA — A powerful method for analyze ecological niches, p. 127–142. In Sanguansat, P. (ed.), *Principal Component Analysis — Multidisciplinary Applications*. InTech, Rijeka. <https://doi.org/10.5772/38538>
- Jolliffe, I.T. 2002. *Principal Component Analysis*. Springer, New York. <https://doi.org/10.1007/b98835>
- Kriwet, J., Mewis, H., and Hampe, O. 2015. A partial skeleton of a new lamniform mackerel shark from the Miocene of Europe. *Acta Palaeontologica Polonica*, 60(4):857–875. <https://doi.org/10.4202/app.00066.2014>
- Legendre, P. and Legendre, L. 1998. *Numerical Ecology*, Second Edition. Elsevier, Amsterdam.
- Maderbacher, M., Bauer, C., Herler, J., Postl, L., Makasa, L., and Sturmbauer, C. 2008. Assessment of traditional versus geometric morphometrics for discriminating populations of the *Tropheus moorii* species complex (Teleostei: Cichlidae), a Lake Tanganyika model for allopatric speciation. *Journal of Zoological Systematics and Evolutionary Research*, 46(2):153–161. <https://doi.org/10.1111/j.1439-0469.2007.00447.x>
- Maisch, H.M., Becker, M.A., Raines, B.W., and Chamberlain, J.A. 2014. Chondrichthyans from the Tallahatta-Lisbon Formation contact (Middle Eocene), Silas, Choctaw County, Alabama. *Paludicola*, 9(4):183–209.

- Marramà, G. and Carnevale, G. 2017. Morphology, relationships and paleobiology of the Eocene barracudina †*Holosteus esocinus* (Aulopiformes, Paralepididae) from Monte Bolca, Italy. *Zoological Journal of the Linnean Society*, 181(1):209– 228.  
<https://doi.org/10.1093/zoolinnean/zlw029>
- Marramà, G. and Kriwet, J. 2017. Principal component and discriminant analyses as powerful tools to support taxonomic identification and their use for functional and phylogenetic signal detection of isolated fossil shark teeth. *PLoS ONE*, 12(11):e0188806.  
<https://doi.org/10.1371/journal.pone.0188806>
- Marramà, G., Bannikov, A.F., Tyler, J.C., Zorzin, R., and Carnevale, G. 2016. Controlled excavations in the Pesciara and Monte Postale sites provide new insights about the paleoecology and taphonomy of the fish assemblages of the Eocene Bolca Konservat-Lagerstätte, Italy. *Palaeogeography, Palaeoclimatology, Palaeoecology*, 454:228–245.  
<https://doi.org/10.1016/j.palaeo.2016.04.021>
- Marramà, G., Carnevale, G., Engelbrecht, A., Claeson, K.M., Zorzin, R., Fornasiero, M., and Kriwet, J. 2017. A synoptic review of the Eocene (Ypresian) cartilaginous fishes (Chondrichthyes: Holocephali, Elasmobranchii) of the Bolca Konservat-Lagerstätte, Italy. *Paläontologische Zeitschrift*, 92(2):283–313.  
<https://doi.org/10.1007/s12542-017-0387-z>
- Marramà, G., Engelbrecht, A., Mörs, T., Reguero, M.A., and Kriwet, J. 2018. The southernmost occurrence of *Brachycarcharias* (Lamniformes, Odontaspidae) from the Eocene of Antarctica provides new information about the paleobiogeography and paleobiology of Paleogene sand tiger sharks. *Rivista Italiana di Paleontologia e Stratigrafia*, 124(2):283–298.  
<https://doi.org/10.13130/2039-4942/9985>
- Marramà, G., Engelbrecht, A., Carnevale, G., and Kriwet, J. 2019. Eocene sand tiger sharks (Lamniformes, Odontaspidae) from the Bolca Konservat-Lagerstätte, Italy: palaeobiology, palaeobiogeography and evolutionary significance. *Historical Biology*, 31(2):102–116.  
<https://doi.org/10.1080/08912963.2017.1341503>
- Marramà, G., Villalobos-Segura, E., Zorzin, R., Kriwet, J., and Carnevale, G. 2023. The evolutionary origin of the durophagous pelagic stingray ecomorph. *Palaeontology*, 66(4):e12669.  
<https://doi.org/10.1111/pala.12669>
- Mitteroecker, P. and Gunz, P. 2009. Advances in geometric morphometrics. *Evolutionary Biology*, 36(2):235–247.  
<https://doi.org/10.1007/s11692-009-9055-x>
- Nyberg, K.G., Ciampaglio, C.N., and Wray, G.A. 2006. Tracing the ancestry of the great white shark, *Carcharodon carcharias*, using morphometric analyses of fossil teeth. *Journal of Vertebrate Paleontology*, 26(4):806–814.  
[https://doi.org/10.1671/0272-4634\(2006\)26\[806:ttaotg\]2.0.co;2](https://doi.org/10.1671/0272-4634(2006)26[806:ttaotg]2.0.co;2)
- Paillard, A., Shimada, K., and Pimiento, C. 2021. The fossil record of extant elasmobranchs. *Journal of Fish Biology*, 98(2):445–455.  
<https://doi.org/10.1111/jfb.14588>
- Pimiento, C., Cantalapiedra, J.L., Shimada, K., Field, D.J., and Smaers, J.B. 2019. Evolutionary pathways toward gigantism in sharks and rays. *Evolution*, 73(3):588–599.  
<https://doi.org/10.1111/evo.13680>
- Purdy, R.W. and Francis, M.P. 2007. Ontogenetic development of teeth in *Lamna nasus* (Bonnaterre, 1758) (Chondrichthyes: Lamnidae) and its implications for the study of fossil shark teeth. *Journal of Vertebrate Paleontology*, 27(4):798–810.  
[https://doi.org/10.1671/0272-4634\(2007\)27\[798:odotil\]2.0.co;2](https://doi.org/10.1671/0272-4634(2007)27[798:odotil]2.0.co;2)
- Robertson, M.P., Caithness, N., and Villet, M.H. 2001. A PCA-based modelling technique for predicting environmental suitability for organisms from presence records. *Diversity and Distributions*, 7(1):15–27. <https://doi.org/10.1046/j.1472-4642.2001.00094.x>
- Rohlf, F.J. 1993. Relative warp analysis and an example of its application to mosquito wings, p. 131–159. In Marcus, L., Bello, E., and García-Valdecasas, A. (eds.), *Contributions to Morphometrics*. Museo Nacional de Ciencias Naturales, Madrid.
- Rohlf, F.J. 2003. TpsRehw, relative warps analysis, version 1.36. Department of Ecology and Evolution, State University of New York at Stony Brook.
- Rohlf, F.J. 2005. TpsDig, digitize landmarks and outlines, version 2.05. Department of Ecology and Evolution, State University of New York at Stony Brook.

- Rohlf, F.J. and Marcus, L.F. 1993. A revolution morphometrics. Trends in Ecology and Evolution, 8(4):129–132.  
[https://doi.org/10.1016/0169-5347\(93\)90024-j](https://doi.org/10.1016/0169-5347(93)90024-j)
- Whitenack, L.B. and Gottfried, M.D. 2010. A morphometric approach for addressing tooth-based species delimitation in fossil mako sharks, *Isurus* (Elasmobranchii: Lamniformes). Journal of Vertebrate Paleontology, 30(1):17–25.  
<https://doi.org/10.1080/02724630903409055>
- Zelditch, M.L., Swiderski, D.L., Sheets, H.D., and Fink, W.L. 2004. Geometric Morphometrics for Biologists: A Primer. Elsevier, Amsterdam.  
<https://doi.org/10.1016/b978-0-12-778460-1.x5000-5>

**APPENDIX 1.**

List of the 120 specimens used in this study with relative locality, age, repository number and position in the jaws. Institutional abbreviations: MC, Massimo Cerato's registered collection, Italy; MCSNV, Museo Civico di Storia Naturale di Verona; MNU, Museum für Natur und Umwelt, Lübeck; NHMUK, Natural History Museum of London; NHMW, Naturhistorisches Museum of Vienna; NRM-PZ, Swedish Natural History Museum, Stockholm; SMNK, State Museum of Natural History, Karlsruhe; SMNS, State Museum of Natural History, Stuttgart; ZC UniVie, Zoological Collection, Department of Palaeontology, University of Vienna. This file can be downloaded as a spreadsheet from:

<https://palaeo-electronica.org/content/2025/5603-geometric-morphometrics-on-fossil-shark-teeth>

Taxon	Repository number	Locality	Age	Position
<i>Brachycarcharias lerichei</i>	MC 89	Bolca Konservat-Lagerstätte, Italy	Eocene	upper antero-lateral
<i>Brachycarcharias lerichei</i>	MCSNV IG.135777	Bolca Konservat-Lagerstätte, Italy	Eocene	lower antero-lateral
<i>Brachycarcharias lerichei</i>	MCSNV IG.135779	Bolca Konservat-Lagerstätte, Italy	Eocene	lower antero-lateral
<i>Brachycarcharias lerichei</i>	MCSNV IG.23598	Bolca Konservat-Lagerstätte, Italy	Eocene	upper lateral
<i>Brachycarcharias lerichei</i>	MCSNV IG.VR.69484	Bolca Konservat-Lagerstätte, Italy	Eocene	upper lateral
<i>Brachycarcharias lerichei</i>	MCSNV IG.VR.69800	Bolca Konservat-Lagerstätte, Italy	Eocene	anterior
<i>Brachycarcharias lerichei</i>	MCSNV T.176	Bolca Konservat-Lagerstätte, Italy	Eocene	upper lateral
<i>Brachycarcharias lerichei</i>	NHMUK PV.OR.43450	Bolca Konservat-Lagerstätte, Italy	Eocene	anterior
<i>Brachycarcharias lerichei</i>	NRM-PZ P15772	Seymour Island, Antarctica	Eocene	upper antero-lateral
<i>Brachycarcharias lerichei</i>	NRM-PZ P15773	Seymour Island, Antarctica	Eocene	upper lateral
<i>Brachycarcharias lerichei</i>	NRM-PZ P15777	Seymour Island, Antarctica	Eocene	lower antero-lateral
<i>Brachycarcharias lerichei</i>	NRM-PZ P15779	Seymour Island, Antarctica	Eocene	lower antero-lateral
<i>Brachycarcharias lerichei</i>	NRM-PZ P15796	Seymour Island, Antarctica	Eocene	upper lateral
<i>Brachycarcharias lerichei</i>	NRM-PZ P15836	Seymour Island, Antarctica	Eocene	upper antero-lateral
<i>Brachycarcharias lerichei</i>	NRM-PZ P15841	Seymour Island, Antarctica	Eocene	upper lateralmost
<i>Brachycarcharias lerichei</i>	NRM-PZ P15848	Seymour Island, Antarctica	Eocene	upper lateral
<i>Brachycarcharias lerichei</i>	NRM-PZ P15857	Seymour Island, Antarctica	Eocene	upper lateral
<i>Brachycarcharias lerichei</i>	NRM-PZ P15888	Seymour Island, Antarctica	Eocene	lower lateral
<i>Carcharias acutissima</i>	SMNS 80739.74	Frauenweiler, Germany	Oligocene	upper lateral
<i>Carcharias acutissima</i>	SMNS 87457.312	Frauenweiler, Germany	Oligocene	upper lateral
<i>Carcharias acutissima</i>	SMNS 87457.321	Frauenweiler, Germany	Oligocene	upper lateral
<i>Carcharias acutissima</i>	SMNS 87457.322	Frauenweiler, Germany	Oligocene	anterior
<i>Carcharias acutissima</i>	SMNS 87457.324	Frauenweiler, Germany	Oligocene	lateralmost
<i>Carcharias cuspidata</i>	SMNK Pal.6598c	Frauenweiler, Germany	Oligocene	anterior
<i>Carcharias cuspidata</i>	SMNK Pal.6598d	Frauenweiler, Germany	Oligocene	lower or upper lateral
<i>Carcharias cuspidata</i>	SMNS 80740.13	Frauenweiler, Germany	Oligocene	anterior
<i>Carcharias cuspidata</i>	SMNS 87457.301	Frauenweiler, Germany	Oligocene	anterior
<i>Carcharias cuspidata</i>	SMNS 87457.302	Frauenweiler, Germany	Oligocene	lower lateral or anterior
<i>Carcharias cuspidata</i>	SMNS 87457.303	Frauenweiler, Germany	Oligocene	anterior
<i>Carcharias cuspidata</i>	SMNS 87457.304	Frauenweiler, Germany	Oligocene	anterior
<i>Carcharias cuspidata</i>	SMNS 87457.305	Frauenweiler, Germany	Oligocene	anterior
<i>Carcharias gustrowensis</i>	SMNS 87457.311	Frauenweiler, Germany	Oligocene	upper lateral
<i>Carcharias taurus</i> (juvenile)	NHMW 98950	-	recent	lower anterior
<i>Carcharias taurus</i> (juvenile)	NHMW 98950	-	recent	lower anterior
<i>Carcharias taurus</i> (juvenile)	NHMW 98950	-	recent	lower anterior

Taxon	Repository number	Locality	Age	Position
<i>Carcharias taurus</i> (juvenile)	NHMW 98950	-	recent	lower lateral
<i>Carcharias taurus</i> (juvenile)	NHMW 98950	-	recent	lower lateral
<i>Carcharias taurus</i> (juvenile)	NHMW 98950	-	recent	lower lateral
<i>Carcharias taurus</i> (juvenile)	NHMW 98950	-	recent	lower lateral
<i>Carcharias taurus</i> (juvenile)	NHMW 98950	-	recent	lower lateral
<i>Carcharias taurus</i> (juvenile)	NHMW 98950	-	recent	lower lateral
<i>Carcharias taurus</i> (juvenile)	NHMW 98950	-	recent	lower lateral
<i>Carcharias taurus</i> (juvenile)	NHMW 98950	-	recent	lower lateral
<i>Carcharias taurus</i> (juvenile)	NHMW 98950	-	recent	lower lateral
<i>Carcharias taurus</i> (juvenile)	NHMW 98950	-	recent	lower lateral
<i>Carcharias taurus</i> (juvenile)	NHMW 98950	-	recent	lower lateral
<i>Carcharias taurus</i> (juvenile)	NHMW 98950	-	recent	lower lateral
<i>Carcharias taurus</i> (juvenile)	NHMW 98950	-	recent	upper anterior
<i>Carcharias taurus</i> (juvenile)	NHMW 98950	-	recent	upper anterior
<i>Carcharias taurus</i> (juvenile)	NHMW 98950	-	recent	upper anterior
<i>Carcharias taurus</i> (juvenile)	NHMW 98950	-	recent	upper lateral
<i>Carcharias taurus</i> (juvenile)	NHMW 98950	-	recent	upper lateral
<i>Carcharias taurus</i> (juvenile)	NHMW 98950	-	recent	upper lateral
<i>Carcharias taurus</i> (juvenile)	NHMW 98950	-	recent	upper lateral
<i>Carcharias taurus</i> (juvenile)	NHMW 98950	-	recent	upper lateral
<i>Carcharias taurus</i> (juvenile)	NHMW 98950	-	recent	upper lateral
<i>Carcharias taurus</i> (juvenile)	NHMW 98950	-	recent	upper lateral
<i>Carcharias taurus</i> (juvenile)	NHMW 98950	-	recent	upper lateral
<i>Carcharias taurus</i> (juvenile)	NHMW 98950	-	recent	upper lateral
<i>Carcharias taurus</i> (juvenile)	NHMW 98950	-	recent	upper lateral
<i>Carcharomodus escheri</i>	MNU 071-20_10E	Groß Pampau, Germany	Miocene	upper lateral
<i>Carcharomodus escheri</i>	MNU 071-20_10H	Groß Pampau, Germany	Miocene	upper lateral
<i>Carcharomodus escheri</i>	MNU 071-20_11A	Groß Pampau, Germany	Miocene	lower anterior
<i>Carcharomodus escheri</i>	MNU 071-20_11D	Groß Pampau, Germany	Miocene	lower lateral
<i>Carcharomodus escheri</i>	MNU 071-20_11E	Groß Pampau, Germany	Miocene	lower lateral
<i>Carcharomodus escheri</i>	MNU 071-20_11F	Groß Pampau, Germany	Miocene	lower lateral
<i>Carcharomodus escheri</i>	MNU 071-20_11G	Groß Pampau, Germany	Miocene	lower lateral
<i>Carcharomodus escheri</i>	MNU 071-20_11H	Groß Pampau, Germany	Miocene	lower lateral
<i>Lamna nasus</i> (adult)	ZC UniVie_2016_1	-	recent	lower anterior
<i>Lamna nasus</i> (adult)	ZC UniVie_2016_1	-	recent	lower anterior
<i>Lamna nasus</i> (adult)	ZC UniVie_2016_1	-	recent	lower anterior
<i>Lamna nasus</i> (adult)	ZC UniVie_2016_1	-	recent	lower anterior
<i>Lamna nasus</i> (adult)	ZC UniVie_2016_1	-	recent	lower lateral
<i>Lamna nasus</i> (adult)	ZC UniVie_2016_1	-	recent	lower lateral
<i>Lamna nasus</i> (adult)	ZC UniVie_2016_1	-	recent	lower lateral
<i>Lamna nasus</i> (adult)	ZC UniVie_2016_1	-	recent	lower lateral
<i>Lamna nasus</i> (adult)	ZC UniVie_2016_1	-	recent	lower lateral
<i>Lamna nasus</i> (adult)	ZC UniVie_2016_1	-	recent	lower lateral
<i>Lamna nasus</i> (adult)	ZC UniVie_2016_1	-	recent	lower lateral
<i>Lamna nasus</i> (adult)	ZC UniVie_2016_1	-	recent	lower lateral
<i>Lamna nasus</i> (adult)	ZC UniVie_2016_1	-	recent	lower lateral
<i>Lamna nasus</i> (adult)	ZC UniVie_2016_1	-	recent	lower lateral
<i>Lamna nasus</i> (adult)	ZC UniVie_2016_1	-	recent	lower lateral
<i>Lamna nasus</i> (adult)	ZC UniVie_2016_1	-	recent	lower lateral
<i>Lamna nasus</i> (adult)	ZC UniVie_2016_1	-	recent	upper anterior

